Dalton Transactions

Accepted Manuscript

ROYAL SOCIETY OF CHEMISTRY

www.rsc.org/dalton

Journal Name

ARTICLE

Heteronuclear Ni(II)-Ln(III) (Ln = La, Pr, Tb, Dy) complexes: Synthesis and Single-Molecule Magnet Behaviour

Received 00th January 20xx,
Accepted 00th January 20xx

DOI: 10.1039/x0xx00000x

www.rsc.org/

Apoorva Upadhyay,[a] Chinmoy Das,[a] Stuart K Langley,[b] Keith S Murray[c], Anant K. Srivastava [d] and Maheswaran Shanmugam[a*]

Abstract: The reaction of hydrated nickel(II) salts (chloride or nitrate) and various hydrated lanthanide nitrate salts with the Schiff base ligand 2-methoxy-6-[(E)-phenyliminomethyl] phenol (HL) in methanol resulted in the isolation of three isostructural linear heterometallic trinuclear complexes and a heterometallic tetranuclear complex. The molecular structures of these complexes were determined via single crystal X-ray diffraction, revealing molecular structures of formulae $[Ni_2La(L^-)_6](NO_3)_{0.55}(OH)_{0.45}$ (**1**), $[Ni_2Pr(L^-)_6](NO_3)_{0.48}(OH)_{0.52}$ (**2**), $[Ni_2Tb(L^-)_6](NO_3)_{0.5}(Cl)_{0.5}$ (**3**) and $[Ni_2Dy_2(L^-)_2(o\text{-vanillin})_2(CO_3)_2(NO_3)_2(MeOH)_2]$ (**4**). Structural analysis for **1**-**3** reveals that the lanthanide ion is sandwiched between two Ni(II) ions and the Ni…Ln...Ni metallic core displays a linear arrangement, with an average ∠Ni…Ln...Ni bond angle of 179.7°. Analysis of **4** reveals the metal ions are arranged such that two Ni-Dy subunits are bridged by two carbonate ligands via the Dy sites. Direct current magnetic susceptibility measurements for complexes **1-4** reveal that the Ni(II) ions are coupled ferromagnetically with the Tb(III) (**3**) and Dy(III) (**4**) ions, and antiferromagnetically with the Pr(III) ion (**2**). For complex **1** a long range intramolecular ferromagnetic interaction is witnessed between the Ni(II) ions (Ni....Ni = 6.873(9) Å) via a closed shell La(III) ion. The magnetic data of **1** were fitted using the HDVV Hamiltonian revealing the following parameters; $J = +0.46\ cm^{-1}$, $g = 2.245$, $D = +4.91\ cm^{-1}$. Alternating current magnetic susceptibility measurements performed on complexes **2**-**4** revealed that **3** and **4** displayed frequency dependent χ_M'' signals ($H_{ac} = 3.5$ Oe and $H_{dc} = 0$ Oe) which is a characteristic signature of a single-molecule magnet behaviour.

Introduction

Discrete molecular coordination complexes where the orientation of the ground electronic spin state (S) is stabilized by a large Ising or axial magnetic anisotropy (D) leads to slow relaxation of the magnetization vector.[1] The marriage of these parameters results in an anisotropy barrier (U_{eff}) to the reversal of the spin orientation. The relationship between U_{eff} and the S and D parameters is given by $U_{eff} = S^2|D|$ (for integer spin), $(S^2-1/4)|D|$ (for non-integer spin) for transition metal species.[2] In general the larger the anisotropy barrier the longer the relaxation time at a given temperature. Such behaviour, which stems from the molecule itself, is termed single molecule magnetism (SMM).[1] SMM behaviour was discovered in 1993 in a mixed valence dodecanuclear manganese complex - $Mn_{12}OAc$ ($U_{eff} = 50\ cm^{-1}$).[1a, b, 3] Following this discovery numerous reports flooded the literature due to the potential applications in digital information storage,[4] molecular qubits,[5] spintronics[6] and as spin valves.[7] Research into transition metal SMMs, which focussed on the development of large polynuclear clusters, as to maximize the ground state spin value (S), revealed, however, that the S and D parameters are inversely proportional to each other, thus hindering the goal of slow magnetic relaxation being realized at higher blocking temperatures.[4e, 8]

While steps have been made towards maximizing and controlling the magnetic anisotropy in low coordinate transition metal complexes, the chemistry is difficult and is still in its infancy.[9] Other equally promising candidates on the periodic table for maximizing the magnetic anisotropy are the lanthanide group of elements. These elements have therefore received a great deal of recent focus in the research of SMMs. The justification of utilizing such elements was originally witnessed in a mononuclear $[Tb(Pc)_2]^-$ (Pc = phthalocyanine anion) sandwich complex, where the anisotropic barrier, U_{eff}, was determined to be 230 cm^{-1} which was significantly larger than the effective energy barrier estimated for any transition metal complex and remains so to date.[10] Following this

---

[a] *Ms. A. Upadhyay, Mr. C. Das, Dr. M. Shanmugam*
Department of Chemistry
Indian Institute of Technology Bombay
Powai, Mumbai, Maharashtra, India -400076.
E-mail: eswar@chem.iitb.ac.in
[b] *Dr. S. K. Langley*
School of Science and the Environment, Chemistry Division, Manchester Metropolitan University,
Manchester, England.
[c] *Em. Prof. K. S. Murray*
Department of Chemistry
Monash University
Victoria, Clayton, Australia.
[d] *Anant K. Srivastava*
Department of Chemistry, Indian Institute of Science Education and Research,
Pune 411 008, Maharashtra, India

† Crystal structures, supporting magnetic data along with crystallographic information files listed in ESI. CCDC numbers: 1054073-1054075 and 1424758.

discovery, new mono- and poly-nuclear lanthanide containing complexes appeared in the literature with very large U_{eff} values, revealing lanthanide complexes as the most promising path towards observing molecules with longer magnetic relaxation times and at higher temperatures.[4a, 11] However, it has been shown experimentally that the long relaxation times which are expected due to the large anisotropy barrier(s) do not materialize due to fast quantum tunnelling of the magnetization (QTM), which shortcuts the anisotropy barrier.[1c, 10a, b, d, 12] Controlling QTM in lanthanide complexes is a daunting task, however, recent reports by Long and co-workers have shown the importance of enhancing the intramolecular exchange interactions (using radical ligands) to quench/suppress the QTM significantly.[13] A similar reduction of QTM efficiency has been reported in mixed 3d-4f complexes, where the transition metal ion is used to generate strong magnetic exchange with the 4f ion, relative to the almost non-existent interactions observed between 4f-4f ions.[14]

With this in mind, we are therefore investigating the synthesis of a new generation of 3d-4f metal complexes using the 3d metal ion Ni(II) and the Schiff base ligand (2-methoxy-6-[(E)-phenyliminomethyl] phenol, HL). In this article, we report the synthesis of three new isostructural heterometallic trinuclear complexes of general formulae $[Ni^{II}_2Ln^{III}(L^-)_6]^+$ where Ln^{3+} = La (**1**), Pr (**2**), Tb (**3**) and a heterometallic tetranuclear complex of formula $[Ni_2Dy_2(L^-)_2(o\text{-vanillin})_2(CO_3)_2(NO_3)_2(MeOH)_2]$ (**4**) and an investigation of their magnetic properties (*vide infra*).

Results and Discussion

Structural description of complexes 1-3

The reaction of the deprotonated Schiff base ligand L^- with two equivalents of $NiCl_2.6H_2O$ or $Ni(NO_3)_2.6H_2O$ and one equivalent of $Ln(NO_3)_3.xH_2O$ (where Ln(III) = Dy or Tb or Pr or La) in methanol, yielded green single crystals after allowing the solution to stand at 6-7 °C for 3-4 days (see experimental section for the detailed synthetic methods).

Single crystal X-ray experiments revealed that three out of the four complexes are isostructural with a general formula $[Ni^{II}_2Ln^{III}(L^-)_6]^+$ where Ln^{III} = La (**1**), Pr (**2**) and Tb (**3**) though they differ in counter anions. The fourth complex, however differs in composition revealing a molecular formula of $[Ni_2Dy_2(L^-)_2(o\text{-vanillin})_2(CO_3)_2(NO_3)_2(MeOH)_2]$ (**4**). A generalized synthetic strategy used to isolate complexes **1**-**4** is given in Scheme 1. As it was found that complexes **1**-**3** are isostructural, a representative crystal structure is shown as Figure 1A (see also Figure S1 of ESI). Complexes **1**-**3** crystallize in the monoclinic space group *C2/c* (Table 1). The asymmetric unit (ASU) for **1**-**3** contains half the complex, with the lanthanide ion lying on an inversion centre. Compounds **1**–**3** are linear heterometallic trinuclear complexes, containing two Ni(II) and a single Ln(III) ion. The Ln(III) ion is sandwiched between the two Ni(II) ions. These are arranged in a linear fashion with a ∠Ni..Ln..Ni bond angle of 179.90° 179.88(9)°, 179.66(5)° for **1**, **2** and **3** respectively.

Scheme 1. The general synthetic method followed for the isolation of **1**-**4**

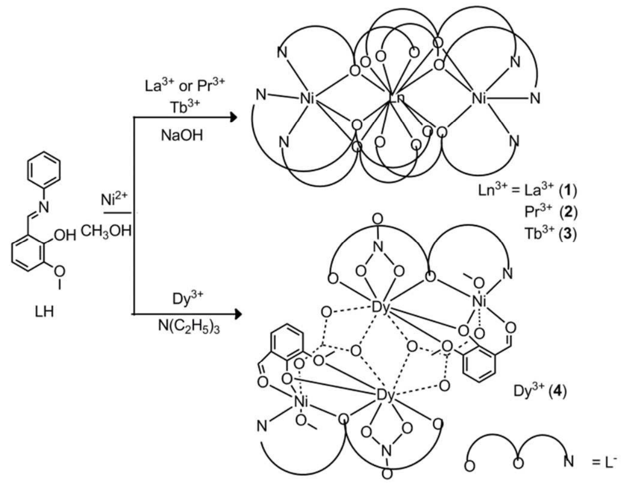

In comparison to **1**–**3**, significant deviations from linearity of the trinuclear Ni…Ln…Ni metallic arrangement have been observed in other related trinuclear complexes when using a Schiff base or other multidentate ligands in the absence of the methoxy group adjacent to the phenoxo group.[15] This strong deviation from linearity is due to the coordination of a chelating nitrate or solvent molecules to the Ln(III) ion.[15b, 16]

Table 1. Crystallographic parameters for complexes **1**-**4**.

	1	**2**	**3**	**4**
Formula	$Ni_2LaC_{84}H_{72}N_{6.45}O_{13.90}$	$Ni_2PrC_{84}H_{72}N_{6.48}O_{13.95}$	$Ni_2TbC_{86}H_{83}N_{6.5}O_{16.5}Cl_{0.5}$	$Ni_2Dy_2C_{48}H_{46}N_4O_{24}$
Size [mm]	0.12 × 0.09 × 0.07	0.13 × 0.11 × 0.08	0.12 × 0.09 × 0.07	0.16 × 0.12 × 0.08
System	Monoclinic	Monoclinic	Monoclinic	Monoclinic
Space group	*C2/c*	*C2/c*	*C2/c*	$P2_1/n$
a [Å]	23.047(3)	22.935(5)	22.819(5)	12.530(5)
b [Å]	23.509(3)	23.393(5)	23.509(6)	12.446(4)
c [Å]	18.570(2)	18.574(4)	18.669(4)	20.918(8)
β [°]	120.378(3)	120.310(4)	119.960(5)	102.904(5)
V [Å^3]	8679.8(18)	8603(3)	8677(4)	3180(2)
Z	4	4	4	2
ρ_{calcd}[g/cm^{-3}]	1.263	1.277	1.352	1.572
$2\Theta_{max}$	53.99	56.68	50.05	55.99
radiation	Mo K_α	Mo K_α	Mo K_α	Mo K_α
λ [Å]	0.71073	0.71073	0.71073	0.71073
T [K]	100(2)	100(2)	100(2)	100(2)
reflns	40058	66136	30422	38888
Ind. reflns	9475	10632	9452	7673
reflns with $I>2\sigma(I)$	6416	7438	7657	7015
R1	0.0486	0.0634	0.0833	0.0726
wR2	0.0818	0.0977	0.1256	0.0802

The three metal ions are stabilized exclusively by six mono-deprotonated ligands. The tridentate ligands enclose the Ni(II) and Ln(III) ions via the imino, phenoxo and methoxy groups. The complexes are mono-cationic with one disordered non-coordinating nitrate anion balancing the charge along with hydroxo (complex **1** and **2**) or chloride ion (complex **3**). The Ni(II) ion exhibits a distorted octahedral geometry with a (N_3O_3) coordination sphere (Figure 2B). The average Ni-N bond length is found to be 2.116(5) Å (for **1**), 2.113(4) Å (for **2**) and 2.126(5) Å (for **3**), while the average Ni-O bond length is found to be 2.047(3) Å (for **1**), 2.045(3) Å (for **2**) and 2.053(4) Å (for **3**). In all three complexes the lanthanide ion displays a distorted Icosahedron geometry with a {LnO_{12}} coordination sphere (Figure 2A). Six out of the twelve sites are derived from phenoxo O-atoms while the remaining six are from the methoxy group. In line with previously reported Ln-O bond lengths, the Ln-O(phenoxo) distances are shorter than the Ln-O(methoxy) bond lengths.[14a, 16b, 17] The average Ln-O (phenoxo) bond distance is found to be 2.524(5) Å (for **1**), 2.481(4) Å (for **2**) and 2.393(4) Å (for **3**) and the Ln-O(methoxy) bond distances are 2.915(5) Å (for **1**), 2.919(4) Å (for **2**) and 2.969(6) Å (for **3**). In all three complexes the Ni(II) ion is linked to the respective lanthanide ion via three phenoxo bridges. The average ∠Ni-O-Ln bond angle is 95.971(5)°, 95.971(5)° and 95.971(5)° for **1**, **2** and **3**, respectively. Selected bond lengths and bond angles for complexes **1**-**3** is given in Table 2.

Following the successful isolation of the heterometallic trinuclear {Ni_2Ln} complexes using the lanthanide ions La, Pr and Tb detailed above, attempts to isolate the analogous Dy complex, the most desirable Ln ion to observe SMM properties, were not successful. Upon maintaining the exact reaction conditions and using $Dy(NO_3)_3.6H_2O$ in place of $Ln(NO_3)_3.6H_2O$ no crystals could be isolated, despite numerous attempts.

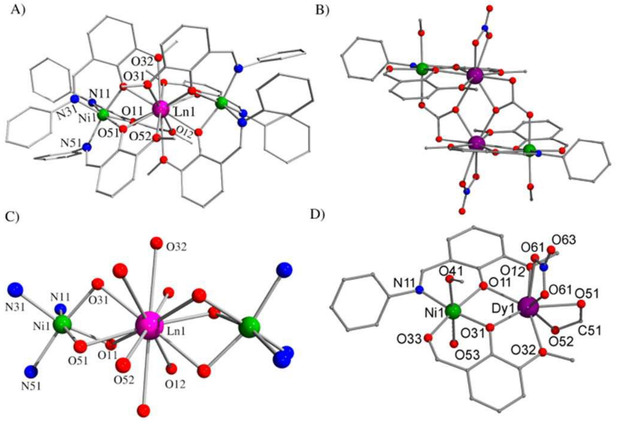

Figure 1. A representative molecular structure of **1-3**. B). Ball and stick representation of the molecular structure of complex **4.** C) The metal core found within **1**-**3**. D) The asymmetric unit of complex **4**. Colour code: Green = Ni(II), Magneta = Ln(III), blue = N, red = O, grey = C

Upon changing the reaction conditions, however, replacing NaOH for Et_3N, and nickel nitrate hydrate in place of nickel halide, crystals could be grown which resulted in the isolation of a new higher nuclearity complex, **4** (Figure 1). Complex **4** was found to be a heterometallic tetranuclear {Ni_2Dy_2} unit which crystallized in the monoclinic space group *P2₁/n*. The ASU of **4** contains half of the molecule (Figure 1D) and the complete molecule is generated by inversion symmetry.

Overall the metallic core of **4** displays two heterobimetallic Ni-Dy units bridged through the Dy ions via two carbonate ligands. The ASU of complex **4** is distinctly different from the ASU found for complexes **1**-**3**. For **4**, the Ni(II) ion is linked to the Dy(III) ion through two μ-phenoxo groups, whereas for **1**-**3** they are bridged via three μ-phenoxo ligands (see Figure 1C and 1D). The average ∠Ni-O-Dy angle and Ni-O-Dy-O dihedral angle in **4** is found to be 103.2° and 10.09°.

Table 2. Selected bond lengths and bond angles for **1**-**3**.

	1 (Å)	**2** (Å)	**3** (Å)
Ln(1)-O(11)	2.517(2)	2.475(3)	2.382(5)
Ln(1)-O(31)	2.525(2)	2.485(3)	2.398(5)
Ln(1)-O(51)	2.525(3)	2.487(3)	2.396(4)
Ln(1)-O(12)	2.937(3)	2.939(5)	2.918(7)
Ln(1)-O(32)	2.919(3)	2.926(4)	2.981(6)
Ln(1)-O(52)	2.892(4)	2.891(6)	2.996(6)
Ni(1)-O(11)	2.047(2)	2.044(3)	2.068(4)
Ni(1)-O(31)	2.041(2)	2.043(3)	2.057(3)
Ni(1)-O(51)	2.052(2)	2.046(2)	2.044(4)
Ni(1)-N(11)	2.122(4)	2.114(4)	2.125(3)
Ni(1)-N(31)	2.116(4)	2.110(3)	2.133(5)
Ni(1)-N(51)	2.118(2)	2.114(3)	2.127(3)
	Bond angle (°)		
Ni(1)-O(11)-Tb(1)	97.135(6)	97.136(11)	95.933(14)
Ni(1)-O(31)-Tb(1)	97.041(6)	96.843(11)	95.743(15)
Ni(1)-O(51)-Tb(1)	96.778(6)	96.692(11)	96.131(15)

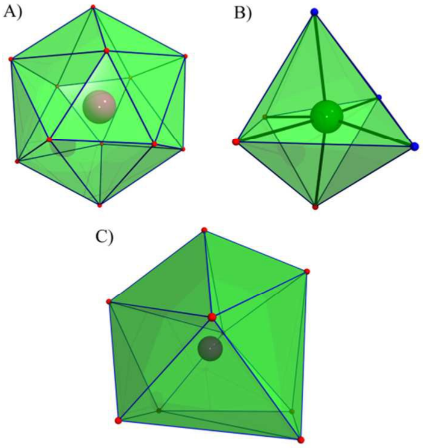

Figure 2. The coordination geometry found around the metal centres in **1**-**3**. A) The distorted icosahedron geometry around the Ln(III) ion in **1**-**3**; B) The distorted octahedral geometry around the Ni(II) ion in **1**-**4**. C) The monocapped square anti-prism coordination geometry exhibited by the Dy(III) ions in **4**.

The drastic change in bond angle, dihedral angle and the number of bridging atoms between the nickel and the dysprosium ions in **4**, compared to **1**-**3** is likely to have a significant influence on the Ni-Ln magnetic exchange interaction and therefore on the magnetization relaxation dynamics (*vide infra*). Of the two phenoxo bridging oxygen atoms one is derived from the deprotonated ligand (L^-), whereas the other is derived from an ortho-vanillin ligand. We note that the free vanillin was not employed during the reaction, and was therefore formed by the *in-situ* hydrolysis of the Schiff base ligand used in the reaction. The coordination environment of the Ni(II) ion is $\{O_5N\}$ and exhibits a pseudo octahedral geometry. Four out of the six coordination sites are provided by L^- and vanillin ligands, with a fifth site occupied by a terminal MeOH solvent molecule. The sixth coordination site of the Ni(II) ion is completed by an oxygen atom of a carbonate ligand. A precursor to incorporate $[CO_3]^{2-}$ ligation in **4** was not employed during the course of the reaction, and is therefore likely to come from the fixation of carbon dioxide from the atmosphere. To confirm the identity of this ligating unit (CO_3^{2-} vs NO_3^-), an infrared (IR) spectrum was measured using KBr pellet (see Figure S2 of ESI). The IR spectrum revealed stretching frequencies at 1554 and 1384 cm^{-1} indicative of coordinated carbonate. Furthermore this evidence is complemented by charge balance considerations.[18] To further confirm this assignment we performed the same reaction under inert conditions (N_2). It was found that crystals of **4** could not be isolated. On the other hand, performing the reaction in the presence of CO_2 gas increased the yield of the reaction to some extent (8%). From this synthetic route it was also found that crystals grew from the filtrate more rapidly compared to when the reaction was performed in aerobic conditions. The carbonate ligand provides a third bridge between the Ni(II) and Dy(III) ions in a μ-η^1-η^1 fashion, which is akin to carboxylate bridging. The average Ni(II)-O and Ni(II)-N bond length in **4** is found to be 2.059 Å and 2.044 Å, respectively.

Table 3. Selected bond length and bond angles for **4**.

	Bond length (Å)		Bond length (Å)
Dy(1)-O(11)	2.303(6)	Ni(1)-O(31)	2.037(6)
Dy(1)-O(52)	2.336(5)	Ni(1)-N(11)	2.044(8)
Dy(1)-O(31)	2.343(6)	Ni(1)-O(33)	2.057(7)
Dy(1)-O(52)#1	2.360(5)	Ni(1)-O(41)	2.088(6)
Dy(1)-O(51)	2.422(6)	Ni(1)-O(53)	2.091(6)
Dy(1)-O(61)	2.474(6)	**Bond angle (°)**	
Dy(1)-O(62)	2.474(6)	Ni(1)-O(31)-Dy(1)	102.3(3)
Dy(1)-O(32)	2.503(6)	Ni(1)-O(11)-Dy(1)	104.1(3)
Dy(1)-O(12)	2.528(6)	Dy(1)-O(52)-Dy#1	116.8(8)
Ni(2)-O(11)	2.024(6)	Dy(1)-O(#52)-Dy#1	116.8(8)

Four out of the nine coordination sites around the Dy(III) ions are provided by two methoxo and phenoxo O-atoms derived from deprotonated L^- and vanillin ligands. Four are completed by chelating nitrate and carbonate ligands, while the final site is provided by a bridging $[CO_3]^{2-}$ ion. The Dy(III) coordination sphere is therefore $\{DyO_9\}$ with a monocapped distorted square anti-prism geometry (Figure 2C). The average Dy-O(phenoxo), Dy-O(methoxo), Dy-O(carbonate) and Dy-O(nitrate) bond lengths are found to be 2.323 Å, 2.516 Å, 2.372 Å and 2.474 Å, respectively. As a consequence of the presence of the $[CO_3]^{2-}$ ligand we find two bridged dinuclear Ni(II)…Dy(III) units, formed, via two μ_4-η^2-η^1-η^1 carbonate ligands, which connect the two Dy(III) ions. The resulting tetranuclear metallic core is therefore strongly influenced by the presence of the carbonate ion. The $\angle$Dy1-O52(carbonate)-Dy#1 bond angle (where Dy#1 represents the symmetrically related atom) is 116.82° (Figure 1B). The Dy1-O52-Dy#1-O#52 atoms lie in the same plane and the dihedral angle is therefore zero. Selected bond lengths and bond angles for complex **4** is shown in Table 3.

Direct current (dc) magnetic susceptibility measurements

Temperature dependent dc magnetic susceptibility measurements were performed on polycrystalline samples of **1**-**4**, between 2 - 300 K and under magnetic fields of 0.1, 0.3 and 0.5 T, respectively (Figure 3). The room temperature (RT) $\chi_M T$ values for **1**-**4** were found to be 2.51, 3.86, 13.76 and 30.8 cm^3 K mol^{-1}, respectively. The observed RT $\chi_M T$ values for **1**-**2** and **4**, are slightly higher than the expected uncoupled value for two Ni(II) and the appropriate Ln(III) ion of 2.0 cm^3 K mol^{-1} (g_{Ni} = 2.0, ligand field term symbol $^3A_2$ for **1**), 3.6 cm^3 K mol^{-1} (g_{Pr} = 4/5, ground state term symbol $^3H_4$, for **2**) 30.33 cm^3 K mol^{-1} (g_{Dy} = 4/3, ground state term symbol: $^6H_{15/2,}$ for **4**). The observed RT value for **3** is slightly lower than the value of 13.81 cm^3 K mol^{-1}(g_{Tb} = 3/2, ground state term symbol: $^7F_6$) for **3** expected for two Ni(II) and one Tb(III) ions that are magnetically uncoupled. The higher value of $\chi_M T$ at RT for **1**, **2** and **4** is common for nickel containing species where the *g*-value of the Ni(II) ion is usually larger than 2.0, due to second order spin-orbit coupling effects.

Upon lowering the temperature each complex reveals distinctly different magnetic behaviour. For **3** and **4**, the $\chi_M T$ value decreases slowly from RT down to 35 K and 19 K, respectively, due to the depopulation of the ligand field split m_J sublevels, which are split on the order of the thermal energy available. Below these temperatures (35 K for **3** and 19 K for **4**), the $\chi_M T$ value increases rapidly reaching a maximum value of 15.86 cm^3 K mol^{-1} at 2.87 K (for **3**) and 26.05 cm^3 K mol^{-1} at 5.0 K (for **4**). The rapid increase in the $\chi_M T$ product is due to ferromagnetic exchange coupling between the Ni(II) ions and the Tb(III) or Dy(III) ions, respectively. This follows the trend of observing ferromagnetic exchange, shown by several other heterodinuclear Ni-Tb or Ni-Dy complexes bridged by two phenoxo or three phenoxo ligands.[14a, 15b, 16c-f, 19] From the available data on Ni-Ln(phenoxo) complexes, it has been found that the magnetic super-exchange interactions are found to be stronger between Ni(II) and lanthanide ions when the double bridged arrangement is present, compared to the situation where three phenoxo groups are bridging (*J* = +4.8 cm^{-1}

(doubly bridged), +0.91 cm^{-1} (triply bridged)).[16c] This was rationalized in 2011 through detailed magneto-structural correlations developed from analogous isotropic Ni-Gd or Ni-Gd-Ni complexes.[20]

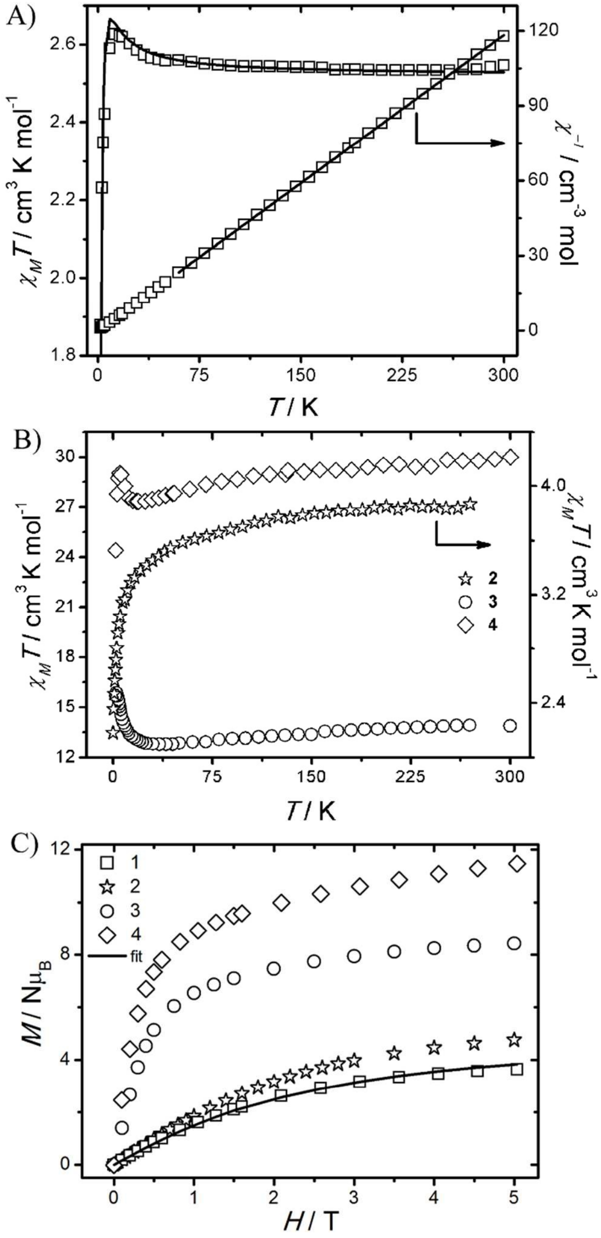

Figure 3. A) Product of temperature and molar magnetic susceptibility as a function of temperature measured at 0.1 Tesla for 1 and the inverse molar susceptibility as a function of temperature. The black solid line shows the best fit obtained for $\chi_M T(T)$ for the parameters discussed in main text. The black solid line in $\chi_M^{-1}(T)$ plot shows the linear fit of the magnetic data from 300 K to 60 K. B) $\chi_M T$ versus T for **2** (0.3 tesla), 3 (0.5 Tesla) and 4 (0.3 Tesla). C) Isothermal field dependant magnetization measurement of **1**-**4** at 2 K. The solid line represents the best fit obtained for **1** using the parameters discussed in main text.

This is an important observation in the context of SMM synthesis, with the extent of the magnetic exchange interaction between the 3d and 4f ions having a significant implication on magnetization relaxation dynamics.[14a, c] It is therefore feasible from these results to design a system using phenoxo based ligands in which a Ni-4f complex displays strong ferromagnetic interactions.

At the lowest temperatures the $\chi_M T$ value drops sharply which could be due to the contributions of multiple factors namely the magnetic anisotropy, intermolecular anti-ferromagnetic interactions and/or dipolar interactions. In contrast to **3** and **4**, the $\chi_M T$ value of **2** decreases gradually from RT down to 50 K before a rapid decrease below this temperature reaching a $\chi_M T$ value of 2.18 cm^3 K mol^{-1} at 1.99 K. This profile indicates antiferromagnetic coupling between the Ni(II) and Pr(III) ions. The antiferromagnetic exchange observed between the Ni(II) and Pr(III) ions has been observed for many other heteronuclear complexes.[16d, 17]

Indeed the nature of the exchange interaction found in both (**3** or **4** and **2)** can be generalized from the empirical evidence available with the following statement. An antiferromagnetic exchange interaction is in general witnessed between Ni(II) {or Cu(II)} ions and a lanthanide ion with a less than a half filled 4f shell and a ferromagnetic interaction is observed when the 4f shell contains seven or more electrons.[15b, 16c-f, 19b, c] It is therefore prudent to utilize the later lanthanide ions when developing Ni(II) based 3d-4f systems.

Due to the presence of first order orbital angular momentum in lanthanide ions, however, extracting the Spin Hamiltonian (SH) parameters by a simple Heisenberg-Dirac-VanVleck (HDVV) method to model the magnetic data of **2**-**4** is difficult. To extract the SH parameter for complexes **2**-**4** further detailed computational calculations are necessary which are currently in progress. The temperature dependent magnetic behaviour of **1** is distinctly different from **2**-**4**. The central lanthanide ion lying between the Ni(II) ions in the trinuclear core is lanthanum(III), which is diamagnetic. The $\chi_M T$ value is temperature independent from RT down to 60 K, suggesting that both the nickel ions behave as simple paramagnets in this temperature regime. This is feasible due to the large intra-nuclear Ni…Ni separation of 6.873(9) Å and any super-exchange interaction needs to be mediated through the diamagnetic La(III) ion.

Below 60 K, however, the $\chi_M T$ value increases steadily reaching a maximum value of 2.60 cm^3 K mol^{-1} at 16 K, suggesting a ferromagnetic exchange interaction between the Ni(II) ions. Kahn and co-workers have shown the existence of long range intramolecular magnetic interactions between paramagnetic Cu(II) ions (Cu(II)…Cu(II); 5.886 Å) in a discrete {Cu$_4$La$_2$} complex mediated via closed-shell rare earth ions.[19a] Indirect evidence for the participation of the diffuse empty La(III) orbitals in the exchange interaction between the Ni(II) ions in **1** can also be understood by considering a 1D-chain constructed from Ni(II) and Na(I) ions using the same Schiff base ligand (L$^-$) reported in this article.[21] These ions are arranged in an alternate Ni-Na-Ni-Na fashion with a Ni(II)…Ni(II) distance being similar to the distance found in complex **1**. In the 1D-chain, no discernible magnetic interactions are observed and a simple paramagnetic signature is witnessed over the entire temperature range.[21] This comparison therefore reveals a system where a diamagnetic La(III) ion is replaced by the alkali metal ion, Na(I), resulting in the interaction between the paramagnetic metal ion(s) being turned off. This emphasizes that the vacant orbital of the diffuse La(III) ion provides a contribution to mediate the ferromagnetic exchange interaction between the Ni(II) ions in **1**.

The inverse magnetic susceptibility data of **1** were fitted from 300 K to 60 K to yield a positive θ value of +0.44 (where θ is Curie-Weiss constant) further supporting the existence of ferromagnetic exchange interaction between the Ni(II) ions (Figure 3A). The steep drop in $\chi_M T$ value below 16 K is likely due to single ion magnetic anisotropy and/or intermolecular antiferromagnetic interaction between the molecules.

The dc magnetic data of **1** were also fitted using PHI software[22] to extract the SH parameters using the HDVV Hamiltonian given below.

$$H = -2JS_{Ni_1}.S_{Ni_2} + 2D_{Ni}S_{Ni_z}^2$$

Attempts to fit the magnetic data (both $\chi_M T(T)$ and $M(H)$ simultaneously) without the inclusion of the zero field splitting parameter D resulted in poor fits of the data. An excellent fit was obtained for $\chi_M T(T)$ data up to 16 K using the parameters J = +0.46 cm^{-1} and an isotropic g-value of 2.245 and D = +4.91 cm^{-1} (Figure 3). Reasonably good fits were obtained for both $\chi_M T(T)$ (over the entire temperature range) and $M(H)$ data simultaneously upon inclusion of the single ion magnetic anisotropy without much deviation in the extracted parameter compared to the above (see Figures S3 and S4, J = +0.46 cm^{-1}, g = 2.245 and D = +4.91 cm^{-1}). Incorporation of intermolecular antiferromagnetic interaction for modelling the magnetic data has no influence on the quality of the fit. The extracted parameters are consistent with the parameters reported in the literature.[16f] The structural distortion is correlated to the magnitude/sign of single ion magnetic anisotropy is elegantly shown by Boča and co-workers in a family of mononuclear Ni(II) complexes (NiN_6; $NiN_4N'_2$, NiN_2O_4, $NiN_2O_2O'_2$) recently,[23] however the developed correlation cannot be applied directly in our system, since Ni(II) ion is surrounded by (O_3N_3) atoms.

Field dependent magnetization measurements were performed up to 5 T for **1** - **4** at 2.0 K (Figure 3C). In all cases a sharp increase in magnetization at low magnetic fields are observed. Upon increasing the external magnetic field the magnetization varies linearly without any clear saturation. The magnetization reaches a final value of 3.61 and 4.75, 8.34, 11.47 $N\mu_B$ at 5 T for complexes **1** - **4**, respectively. The significantly lower magnetization value in comparison to expected values (5.2, 11.0 and 22 $N\mu_B$ for **1**, **2** and **4** respectively) at high magnetic field at 2 K is due to the lifting of degeneracy of m_j levels by the ligand field.

Alternating current (ac) magnetic susceptibility measurements of complexes 2 – 4

Ac magnetic susceptibility measurements were performed with a 3.5 Oe oscillating magnetic field in the temperature range 2-8 K at various frequencies to investigate the magnetization relaxation dynamics of complexes **2**-**4** (Figure 4). For complex **2** no frequency dependent out-of-phase susceptibility (χ_M'') signal is observed in the absence or the presence of a static dc magnetic field. On the other hand, complex **3** shows frequency dependent χ_M'' signals (H_{dc} = 0 Oe), indicating the possibility of SMM behaviour (see Figure S5 of ESI). It is found, however, that the peak maxima needed to extrapolate the relaxation time(s) are found below the operating limit of the magnetometer. This would indicate fast magnetic relaxation a consequence of a small anisotropy barrier U_{eff} or fast QTM or perhaps both. Multiple factors are likely to be responsible for the fast relaxation times (no maxima in χ_M'') for complex **3** in the temperature range probed, namely the strength of the exchange interaction, the distorted symmetry around the Tb(III) ion and the non-Kramers nature of the ion. If QTM is fast, common in Tb(III) systems, then it can often be suppressed by the application of a large static dc field.

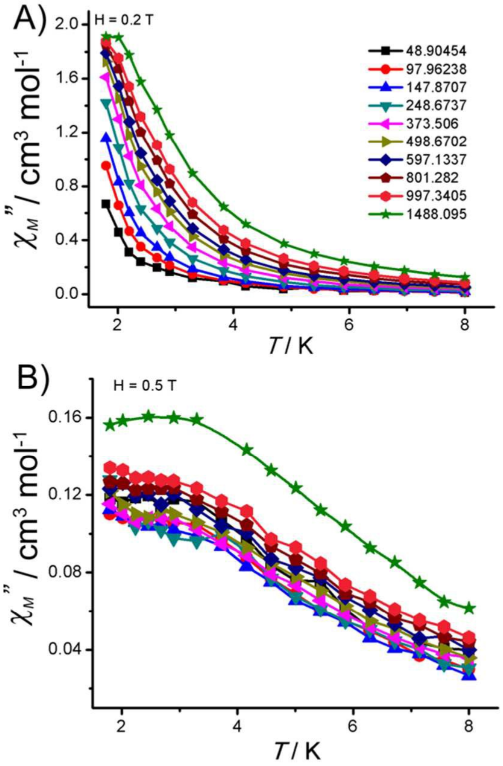

Figure 4. Frequency dependent out-of-phase susceptibility measurements performed on polycrystalline samples of complexes **3** and **4** in the presence of a static dc magnetic field of 0.2 T and 0.5 T.

Magnetization relaxation measurements were therefore performed in the presence of an external static magnetic field

(H_{dc} = 0.2 T), which again failed to reveal any maxima in the $\chi_M''(T)$ plot (Figure 4A). This indicates that the relaxation times are not affected by the application of an external bias field.

A Similar scenario was observed for complex **4**. While out-of-phase susceptibility signals are observed with H_{ac} = 3.5 Oe and H_{dc} = 0 Oe, the χ_M'' maxima were found to be well below the low temperature limit of the instrument (Figure S5 of ESI). This again implies that the magnetization vector changes its orientation extremely fast, likely due to a small anisotropy barrier, fast QTM or a combination of both. Again the application of a static dc magnetic field (H_{dc} = 0.5 T) failed to slow the relaxation time(s).

It has been detailed on several occasions that small changes in the coordination geometry around the Dy(III) ion can have a significant influence on the orientation of magnetic easy axis (g_z) which governs the magnetization relaxation dynamics.[12a, q, 24]

Often advanced and expensive *ab initio* calculations are required to predict the orientation of the easy axis at the Dy(III) sites. A recent article by Chilton and co-workers, however, provided a simple yet elegant electrostatic model that can be utilized to predict the orientation of the g_z axis of various low symmetric Dy(III) ions from the X-ray crystal structure data.[25] This new approach has been tested with many multinuclear Dy(III) complexes and the predicted g_z orientation coincides very well with *ab initio* g-tensor orientation calculations/predictions.[26] The magnetic easy axis orientation of the Dy(III) ions in complex **4** was therefore predicted using this electrostatic model approach through the Magellan software package,[25] and is shown in Figure 5. The crystal field potential constructed from the fractional charges on the coordinating atoms (based on valence bond resonance hybrid model) is shown in Figure 5A. Among the four different ligands coordinated to the Dy(III) ions, the phenoxo oxygen atoms derived from L^- and *o*-Vanillin ligands possess a high negative charge compared to nitrate and carbonate ligands. Moreover the bond distance of the phenoxo atoms are much closer to the Dy(III) ion than the other ligands. The oblate electron density of the Dy(III) will be in a high energy configuration when the quantization axis is normal to these phenoxo bridges, and therefore the minimal electrostatic energy and the anisotropic axis is found to be parallel to the phenoxo bridges. The magnetic easy axis does not coincide with its pseudo molecular C_2 axis confirming that the geometry around the Dy(III) does not have any influence on the orientation of the g_z-axis, which is predominantly governed by the electrostatic potential associated with the ligating atoms.

We have recently reported a $[Ni_2Dy_2]^{3+}$ complex using a Schiff base ligand similar to the ligand used here. This displayed SMM behavior, with an anisotropy barrier of 19 K where the magnetization vector follows predominantly an Orbach relaxation mechanism, with no observable QTM in the temperature range studied.[14a] The coordination environment of the $[Ni_2Dy_2]^{2+}$ complex is very similar to that in **4**, with two phenoxo ligands bridging the Ni-Dy ions, but there is no apical ligands (such as carbonate, nitrate or acetate) are present connecting the ions. Further structural differences are found in that the two [Ni(II)-Dy(III)] dinuclear units are linked via three carboxylate groups in an μ-η^1-η^1 fashion.

As expected in the $[Ni_2Dy_2]^{3+}$ complex, the g_z orientation is parallel (Figure S6 of ESI) to the phenoxo bridges as with **4**, and with this being the case the absence of clear maxima in χ_M'' for **4,** which is clearly present for $[Ni_2Dy_2]^{3+}$, is quite surprising. Since in both complexes, the orientation of g_z axis is very similar, the structural distortion around the metal ions is likely to have a significant influence in magnetization relaxation dynamics. Hence, we analyzed the crystal structure of **4** in detail. In an unrelated report its has been claimed that the strength of exchange interaction between Ni(II) and Dy(III) ions is also determined by the ∠Ni-O(phenoxo)-Dy angle and the Dy-O(phenoxo)-Ni-O(phenoxo) dihedral angle. It was shown that the larger the bond angle and the smaller the dihedral angle favours a strong ferromagnetic exchange interaction. This fact is rationalized by detailed computational calculations on a family of Ni-Gd complexes.[20] The smaller ∠Ni-O(phenoxo)-Dy bond angle (103.2°) and larger distortion in the dihedral plane (10.09°) in **4** compared to the values of 106.7°and 8.8° reported in the $[Ni_2Dy_2]^{3+}$ complex suggests that the Ni-Dy interaction will be smaller for **4** in comparison to $[Ni_2Dy_2]^{3+}$. The presence of the apical carbonate ligand in **4** presumably leads to a significant distortion in Ni-O-Dy-O plane, resulting in weak ferromagnetic exchange between the Ni(II) and Dy(III) ions. Colacio and co-workers have shown the influence of the apical ligand in magnetization relaxation dynamics in a Ni-Dy dimeric complex whose coordination environment is very similar to complex **4**.[19g, h]

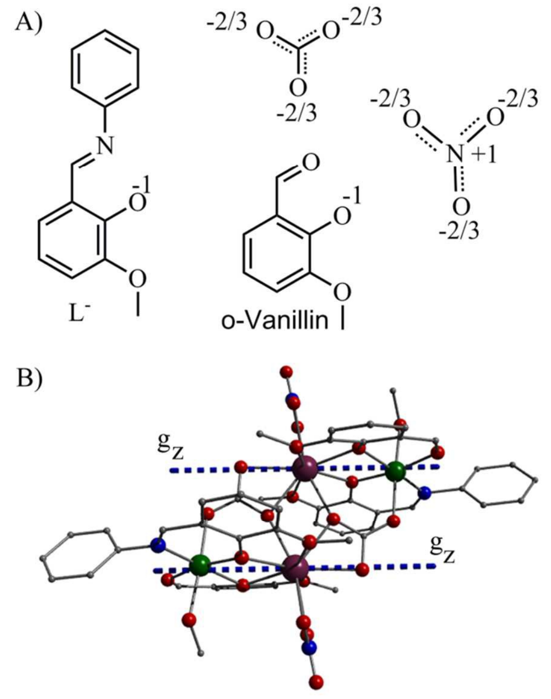

Figure 5. A) Partial charges assigned for the various ligands bound to the Dy(III) ion in **4**. B) The dotted blue line indicates the orientation of magnetic easy axis (g_z) of Dy(III) ions in **4**.

Strength of the exchange interaction between the Ni(II) and Dy(III) in **4** is presumably not sufficient enough to block the under barrier tunneling mechanism and leads to faster magnetic relaxation times compared to the $[Ni_2Dy_2]^{3+}$ complex. The weaker exchange is problematic for two reasons, firstly magnetic relaxation pathways such as zero field and thermally assisted quantum tunneling of the magnetization become efficient and are in direct competition with the Orbach process.[27] Secondly, as shown in a series of $\{Cr_2Dy_2\}$ complexes the smaller exchange interaction provides a smaller thermal energy barrier, compared to complexes with larger 3d-4f exchange values, if the relaxation is of the multi-level exchange type and thus resulting in faster relaxation times.[27-28] The comparison of the two $\{Ni_2Dy_2\}$ complexes with similar but subtly different Ni-Dy dinuclear units revealed differing magnetic relaxation dynamics. The study confirms that even small structural changes in the Dy(III) coordination environment and Ni-Dy bridging motifs have a dramatic influence in magnetization relaxation dynamics in lanthanide based SMMs. Apart from the exchange interaction between the ions (Ni(II) and Dy(III)), other parameters such as intermolecular interactions and dipolar coupling may play a crucial role in magnetization relaxation dynamics. To nail down the individual contribution and to better understand the magnetization relaxation dynamics further detailed studies are required which are currently in progress.

Conclusions

We have isolated three isostructural heterometallic trinuclear complexes of formula $[Ni_2Ln(L^-)_6]^+$where Ln = La (**1**), Pr (**2**) and Tb (**3**) and a tetranuclear $[Ni_2Dy_2(L^-)_2$(*o*-vanillin)$_2(CO_3)_2(NO_3)_2(MeOH)_2]$ (**4**) complex. Compounds **1**-**3** display a linear trimetallic core, with a Ln(III) ion sandwiched between two Ni(II) ions. Complex **4** is derived from two Ni(II)-Dy(III) units which are bridged by two carbonate ligands. Dc magnetic susceptibility measurements revealed that the Ni(II) ions are coupled ferromagnetically with the Tb(III) and Dy(III) ion and antiferromagnetically with the Pr(III) ion. This is in agreement with previously reported data. The data from this study and elsewhere suggests that the magnetic exchange between Ni(II) and Ln(III) follows a predictable trend being that the magnetic exchange interaction is ferromagnetic when the number of 4f electrons is greater than seven and antiferromagnetic when less than seven. Interestingly a weak magnetic ferromagnetic exchange interaction is found between the Ni(II) ions of **1** (J = +0.46 cm^{-1}, g = 2.245, D = +4.91 cm^{-1}) mediated through the diamagnetic lanthanum(III) ion. Alternating current magnetic susceptibility measurements revealed the onset of frequency dependent out-of-phase signals for complex **3** and **4** indicating the possibility of single-molecule magnet behaviour. The assumed weaker exchange interaction between the Ni(II) and Dy(III) ions and the presence of multiple weak exchange pathways through the carbonate and phenoxo bridges in **4** is likely the reason for the observation of faster magnetization relaxation times compared to the structurally similar $[Ni_2Dy_2]^{3+}$.[14a] Detailed theoretical studies are required to understand the electronic structure and to determine whether the relaxation pathway(s) are single ion in origin or of a multi-level exchange type. These calculations are currently in progress.

Experimental Section

Materials and methods

All the reactions were performed under aerobic condition unless otherwise specified. All the chemicals and solvents of analytical grade were purchased from Alfa Aesar and used without any further purification. The Schiff base ligand was synthesized as per the literature.[29] Infrared spectra were recorded for the solid samples using KBr pellets on a Perkin-Elmer FT-IR spectrometer in the 400 to 4000 cm^{-1} range. Magnetic susceptibility measurements were performed on MPMS SQUID magnetometer. Magnetic data were modelled using the PHI software program[22] and the anisotropic axes around the Dy(III) ions were obtained by using Magellan software.[25]

X-ray crystallography

Single crystal data were collected on a Bruker SMART Apex Duo/Rigaku Saturn diffractometer (MoK$_\alpha$, λ = 0.71073 Å). The selected crystals were mounted on a fibre loop using Paratone-N oil and placed in the cold flow produced with an Oxford Cryo-cooling device. Complete hemispheres of data were collected by using ω and φ-scans (0.3 Å, 30 s per frame). Integrated intensities were obtained with SAINT+/Crystal Clear-SM Expert (Rigaku 2012) and they were corrected for absorption using SADABS. Structure solution and refinement was performed with the SHELX-package. The structures were solved by direct methods and completed by iterative cycles of ΔF syntheses and full-matrix least-squares refinement against F^2. It was not possible to solve the diffused electron density residual which was associated with solvent molecules for the complex. This was treated with the SQUEEZE routine from PLATON resulted in smooth convergence of all the atoms during refinement. The loop corresponds to the residual electron density (created in PLATON) is appended in cif file of the complex.

Synthetic procedure of 1

To a 30 mL methanolic solution of HL (0.3 g, 1.3215 mmol) solid sodium hydroxide (0.528 g, 1.321 mmol) was added which was stirred for five minutes for complete deprotonation. Upon deprotonation, the solution changes from orange to yellow. $La(NO_3)_3.6H_2O$ (0.2861 g, 0.6607 mmol) was then added and the resultant mixture was stirred for 15 minutes at room temperature. After 15 minutes, $NiCl_2.6H_2O$ (0.3141 g, 1.3215 mmol) was added resulting in a green solution. The solution was then allowed to stir for 8 hrs at room temperature. After this time the reaction mixture was filtered. The solution was then left undisturbed at 6-7 °C for 3-4 days after which green single crystals suitable for x-ray diffraction formed after 3-4 days. FT-IR (KBr pellet): 2923 cm^{-1} (s, $\nu_{(Ar-H)}$), 1610 cm^{-1} (s, $\nu_{(C=N)}$). Elemental analysis calculated (%) for $C_{84}H_{72}N_{6.45}O_{13.90}Ni_2La$ (**1**) (1652.82): C 61.04, H 4.39, N 5.50;

found: C 60.89, H 4.27, N 5.41. Yield (% based on La^{3+}) = 80 mg (7.22%).

Synthetic procedure of 2 and 3

A similar synthetic procedure for **1** was followed, except La$(NO_3)_3$.xH$_2$O was replaced by Pr$(NO_3)_3$.6H$_2$O (0.2874 g, 0.6607 mmol) in case of **2** and Tb$(NO_3)_3$.xH$_2$O (0.2279 g, 0.6607 mmol) in case of **3**. FT-IR (KBr pellet) for **2**: 2925 cm^{-1} (s, $\nu_{(Ar-H)}$), 1610 cm^{-1} (s, $\nu_{(C=N)}$); for **3**: 2926 cm^{-1} (s, $\nu_{(Ar-H)}$), 1611 cm^{-1} (s, $\nu_{(C=N)}$). Elemental analysis calculated (%) for $C_{84}H_{72}N_{6.48}O_{13.95}Ni_2Pr$ (**2**) (1653.95): C 61.0, H 4.38, N 5.50; found: C 60.20, H 4.22, N 5.32 and for $C_{84}H_{72}N_{6.50}O_{13.5}Cl_{0.5}Ni_2Tb$ (**3**) (1681.84): C 59.98, H 4.31, N 5.40; found: C 60.02, H 4.29, N 5.27. Yield for **2** (% based on Pr^{3+}) = 85 mg (7.7%). Yield for **3** (% based on Tb^{3+}) = 42 mg (3.7%).

Synthetic procedure of 4

To a 30 mL methanolic solution of HL (0.3 g, 1.3215 mmol) equimolar triethylamine (0.0183 ml, 1.321 mmol) was added which was stirred for 10 minutes. Into the above solution Dy$(NO_3)_3$.5H$_2$O (0.2898 g, 0.6607 mmol) was added and the resultant mixture was stirred for a further 15 minutes. After this time Ni$(NO_3)_3$.6H$_2$O (0.3843 g, 1.3215 mmol) was added and the solution changed from light orange to green. The solution was then stirred for 18 hrs at room temperature. After this time the reaction mixture was filtered and the filtrate was left undisturbed for crystallization at 6-7 °C. After 1 week crystals suitable for x-ray diffraction had formed. Elemental analysis calculated (%) for $Ni_2Dy_2C_{48}H_{46}N_4O_{24}$ (1505.3) Calculated (%): C 38.30, H 3.10, N 3.70; found (%): C 38.27, H 3.08, N 3.65. Yield for **4** (% based on Dy^{3+}) = 30 mg (4.05%).

Acknowledgements

MS likes to acknowledge Department of Science and Technology (SR/S1/IC-32/2011), DST Nanomission (SR/NM/NS-1119/2011) and Indian Institute of Technology Bombay for financial support. KSM thanks the Australian Research Council for a Discovery Grant.

Notes and references

Crystallographic information files for all the complexes and supporting magnetic data information are listed in ESI. CCDC numbers: 1054073-1054075 and 1424758.

1 a) R. Sessoli, H. L. Tsai, A. R. Schake, S. Wang, J. B. Vincent, K. Folting, D. Gatteschi, G. Christou and D. N. Hendrickson, *J. Am. Chem. Soc.* 1993, **115**, 1804; b) D. Gatteschi, A. Caneschi, L. Pardi and R. Sessoli, *Science* 1994, **265**, 1054; c) D. Gatteschi and R. Sessoli, *Angew. Chem., Int. Ed.* 2003, **42**, 268.

2 D. Gatteschi, R. Sessoli and J. Villain, *Molecular Nanomagnets*, Oxford Press, **2006**.

3 a) R. Sessoli, D. Gatteschi, A. Caneschi and M. A. Novak, *Nature* 1993, **365**, 141; b) G. Aromi and E. K. Brechin, *Struct. Bonding* 2006, **122**, 1.

4 a) R. J. Blagg, L. Ungur, F. Tuna, J. Speak, P. Comar, D. Collison, W. Wernsdorfer, E. J. L. McInnes, L. F. Chibotaru and R. E. P. Winpenny, *Nat. Chem.* 2013, **5**, 673; b) G. A. Craig and M. Murrie, *Chem. Soc. Rev.* 2015, **44**, 2135; c) F. Habib, I. Korobkov and M. Murugesu, *Dalton Trans.* 2015, **44**, 6368; d) S. Maheswaran, G. Chastanet, S. J. Teat, T. Mallah, R. Sessoli, W. Wernsdorfer and R. E. P. Winpenny, *Angew. Chem., Int. Ed.* 2005, **44**, 5044; e) C. J. Milios, R. Inglis, A. Vinslava, R. Bagai, W. Wernsdorfer, S. Parsons, S. P. Perlepes, G. Christou and E. K. Brechin, *J. Am. Chem. Soc.* 2007, **129**, 12505; f) C. J. Milios, A. Vinslava, W. Wernsdorfer, S. Moggach, S. Parsons, S. P. Perlepes, G. Christou and E. K. Brechin, *J. Am. Chem. Soc.* 2007, **129**, 2754; g) K. M. Poole, M. Korabik, M. Shiddiq, K. J. Mitchell, A. Fournet, Z. You, G. Christou, S. Hill and M. Holynska, *Inorg. Chem.* 2015, **54**, 1883; h) R. Sato, K. Suzuki, T. Minato, M. Shinoe, K. Yamaguchi and N. Mizuno, *Chem. Commun.* 2015, **51**, 4081; i) M. Shanmugam, G. Chastanet, T. Mallah, R. Sessoli, S. J. Teat, G. A. Timco and R. E. P. Winpenny, *Chem. - Eur. J.* 2006, **12**, 8777; j) M. Shanmugam, M. Shanmugam, G. Chastanet, R. Sessoli, T. Mallah, W. Wernsdorfer and R. E. P. Winpenny, *J. Mater. Chem.* 2006, **16**, 2576; k) D. N. Woodruff, R. E. P. Winpenny and R. A. Layfield, *Chem. Rev.* 2013, **113**, 5110; l) P.-F. Zhuang, Y.-J. Zhang, H. Zheng, C.-Q. Jiao, L. Zhao, J.-L. Wang, C. He, C.-Y. Duan and T. Liu, *Dalton Trans.* 2015, **44**, 3393.

5 a) J. J. Baldovi, S. Cardona-Serra, J. M. Clemente-Juan, E. Coronado, A. Gaita-Arino and A. Palii, *Inorg. Chem.* 2012, **51**, 12565; b) M. J. Martinez-Perez, S. Cardona-Serra, C. Schlegel, F. Moro, P. J. Alonso, H. Prima-Garcia, J. M. Clemente-Juan, M. Evangelisti, A. Gaita-Arino, J. Sese, J. van Slageren, E. Coronado and F. Luis, *Phys. Rev. Lett.* 2012, **108**, 247211; c) G. Gonzalez and M. N. Leuenberger, *Handb. Nanophys.* 2011, **6**, 1; d) M. Affronte, F. Troiani, A. Ghirri, A. Candini, M. Evangelisti, V. Corradini, S. Carretta, P. Santini, G. Amoretti, F. Tuna, G. Timco and R. E. P. Winpenny, *J. Phys. D Appl. Phys.* 2007, **40**, 2999; e) M. Affronte, F. Troiani, A. Ghirri, S. Carretta, P. Santini, V. Corradini, R. Schuecker, C. Muryn, G. Timco and R. E. Winpenny, *Dalton Trans.* 2006, 2810; f) M. Affronte, F. Troiani, A. Ghirri, S. Carretta, P. Santini, R. Schuecker, G. Timco and R. E. P. Winpenny, *J. Magn. Magn. Mater.* 2007, **310**, e501; g) F. Troiani, A. Ghirri, M. Affronte, S. Carretta, P. Santini, G. Amoretti, S. Piligkos, G. Timco and R. E. P. Winpenny, *Phys. Rev. Lett.* 2005, **94**, 207201; h) C. J. Wedge, G. A. Timco, E. T. Spielberg, R. E. George, F. Tuna, S. Rigby, E. J. L. McInnes, R. E. P. Winpenny, S. J. Blundell and A. Ardavan, *Phys. Rev. Lett.* 2012, **108**, 107201.

6 a) J. M. Clemente-Juan, E. Coronado and A. Gaita-Arino, *Chem. Soc. Rev.* 2012, **41**, 7464; b) R. E. P. Winpenny, *Nat. Nanotechnol.* 2013, **8**, 159.

7 F. R. Renani and G. Kirczenow, *Phys. Rev. B Condens. Matter Mater. Phys.* 2013, **87**, 121401.

8 a) G. Rigaux, R. Inglis, S. Morrison, A. Prescimone, C. Cadiou, M. Evangelisti and E. K. Brechin, *Dalton Trans.* 2011, **40**, 4797; b) A. M. Ako, I. J. Hewitt, V. Mereacre, R. Clerac, W. Wernsdorfer, C. E. Anson and A. K. Powell, *Angew. Chem., Int. Ed.* 2006, **45**, 4926; c) A. M. Ako, Y. Lan, O. Hampe, E. Cremades, E. Ruiz, C. E. Anson and A. K. Powell, *Chem. Commun.* 2014, **50**, 5847; d) A. M. Ako, V. Mereacre, R. Clerac, W. Wernsdorfer, I. J. Hewitt, C. E. Anson and A. K. Powell, *Chem. Commun.* 2009, 544.

9 a) M. Atanasov, J. M. Zadrozny, J. R. Long and F. Neese, *Chem. Sci.* 2013, **4**, 139; b) J. M. Zadrozny, M. Atanasov, A. M. Bryan, C.-Y. Lin, B. D. Rekken, P. P. Power, F. Neese and J. R. Long, *Chem. Sci.* 2013, **4**, 125; c) J. M. Zadrozny, D. J. Xiao, M. Atanasov, G. J. Long, F. Grandjean, F. Neese and J. R. Long, *Nat. Chem.* 2013, **5**, 577; d) R. C. Poulten, M. J. Page, A. G. Algarra, J. J. Le Roy, I. Lopez, E. Carter, A. Llobet, S. A. Macgregor, M. F. Mahon, D. M. Murphy, M. Murugesu and M. K. Whittlesey, *J. Am. Chem. Soc.* 2013, **135**, 13640; e) S. Vaidya, A. Upadhyay, K. Singh Saurabh, T. Gupta, S. Tewary, K. Langley Stuart, P. S. Walsh James, S. Murray Keith, G. Rajaraman and M. Shanmugam, *Chem Commun* 2015, **51**, 3739.

10 a) N. Ishikawa, *Polyhedron* 2007, **26**, 2147; b) N. Ishikawa, M. Sugita, T. Ishikawa, S.-Y. Koshihara and Y. Kaizu, *J. Am. Chem. Soc.* 2003, **125**, 8694; c) N. Ishikawa, M. Sugita, N. Tanaka, T.

Ishikawa, S.-Y. Koshihara and Y. Kaizu, *Inorg. Chem.* 2004, **43**, 5498; d) N. Ishikawa, M. Sugita and W. Wernsdorfer, *J. Am. Chem. Soc.* 2005, **127**, 3650.

11 a) J. Le Roy Jennifer, I. Korobkov and M. Murugesu, *Chem Commun* 2014, **50**, 1602; b) J. Le Roy Jennifer, L. Ungur, I. Korobkov, F. Chibotaru Liviu and M. Murugesu, *J Am Chem Soc* 2014, **136**, 8003; c) L. Ungur, J. J. Le Roy, I. Korobkov, M. Murugesu and L. F. Chibotaru, *Angew. Chem., Int. Ed.* 2014, **53**, 4413.

12 a) D. Gatteschi and R. Sessoli, *Angew. Chem., Int. Ed.* 2003, **42**, 268; b) M. A. AlDamen, S. Cardona-Serra, J. M. Clemente-Juan, E. Coronado, A. Gaita-Arino, C. Marti-Gastaldo, F. Luis and O. Montero, *Inorg. Chem.* 2009, **48**, 3467; c) M. A. AlDamen, J. M. Clemente-Juan, E. Coronado, C. Marti-Gastaldo and A. Gaita-Arino, *J. Am. Chem. Soc.* 2008, **130**, 8874; d) P. Bag, C. K. Rastogi, S. Biswas, S. Sivakumar, V. Mereacre and V. Chandrasekhar, *Dalton Trans.* 2015, **44**, 4328; e) S. Biswas, S. Das, J. van Leusen, P. Koegerler and V. Chandrasekhar, *Eur. J. Inorg. Chem.* 2014, 4159; f) S. Cardona-Serra, J. M. Clemente-Juan, E. Coronado, A. Gaita-Arino, A. Camon, M. Evangelisti, F. Luis, M. J. Martinez-Perez and J. Sese, *J. Am. Chem. Soc.* 2012, **134**, 14982; g) C. Das, A. Upadhyay, S. Vaidya, S. K. Singh, G. Rajaraman and M. Shanmugam, *Chem. Commun.* 2015, **51**, 6137 ; h) S. Das, A. Dey, S. Biswas, E. Colacio and V. Chandrasekhar, *Inorg. Chem.* 2014, **53**, 3417; i) S. Das, S. Hossain, A. Dey, S. Biswas, J.-P. Sutter and V. Chandrasekhar, *Inorg. Chem.* 2014, **53**, 5020; j) S. Demir, M. Nippe, M. I. Gonzalez and J. R. Long, *Chem. Sci.* 2014, **5**, 4701; k) S. Demir, J. M. Zadrozny and J. R. Long, *Chem. - Eur. J.* 2014, **20**, 9524; l) P.-H. Guo, Y. Meng, Y.-C. Chen, Q.-W. Li, B.-Y. Wang, J.-D. Leng, D.-H. Bao, J.-H. Jia and M.-L. Tong, *J. Mater. Chem. C* 2014, **2**, 8858; m) T. Gupta and G. Rajaraman, *J. Chem. Sci.* 2014, **126**, 1569; n) W. Huang, J. J. Le Roy, S. I. Khan, L. Ungur, M. Murugesu and P. L. Diaconescu, *Inorg. Chem.* 2015, **54**, 2374; o) L.-L. Li, S. Liu, Y. Zhang, W. Shi and P. Cheng, *Dalton Trans.* 2015, **44**, 6118; p) R. Marx, F. Moro, M. Doerfel, L. Ungur, M. Waters, S. D. Jiang, M. Orlita, J. Taylor, W. Frey, L. F. Chibotaru and J. van Slageren, *Chem. Sci.* 2014, **5**, 3287; q) E. Moreno Pineda, N. F. Chilton, R. Marx, M. Dorfel, D. O. Sells, P. Neugebauer, S.-D. Jiang, D. Collison, J. van Slageren, E. J. L. McInnes and R. E. P. Winpenny, *Nat. Commun.* 2014, **5**, 5243; r) S. K. Singh, T. Gupta and G. Rajaraman, *Inorg. Chem.* 2014, **53**, 10835; s) S. K. Singh, T. Gupta, M. Shanmugam and G. Rajaraman, *Chem. Commun.* 2014, **50**, 15513; t) L. Ungur, S.-Y. Lin, J. Tang and L. F. Chibotaru, *Chem. Soc. Rev.* 2014, **43**, 6894; u) P. Zhang, L. Zhang and J. Tang, *Dalton Trans.* 2015, **44**, 3923; v) H.-H. Zou, L.-B. Sheng, Z.-L. Chen and F.-P. Liang, *Polyhedron* 2015, **88**, 110.

13 a) J. D. Rinehart, M. Fang, W. J. Evans and J. R. Long, *J. Am. Chem. Soc.* 2011, **133**, 14236; b) J. D. Rinehart, M. Fang, W. J. Evans and J. R. Long, *Nat. Chem.* 2011, **3**, 538.

14 a) N. Ahmed, C. Das, S. Vaidya, S. K. Langley, K. S. Murray and M. Shanmugam, *Chem. - Eur. J.* 2014, **20**, 14235; b) S. K. Langley, D. P. Wielechowski, V. Vieru, N. F. Chilton, B. Moubaraki, B. F. Abrahams, L. F. Chibotaru and K. S. Murray, *Angew. Chem., Int. Ed.* 2013, **52**, 12014; c) S. K. Langley, D. P. Wielechowski, V. Vieru, N. F. Chilton, B. Moubaraki, L. F. Chibotaru and K. S. Murray, *Chem. Sci.* 2014, **5**, 3246.

15 a) C. G. Efthymiou, A. N. Georgopoulou, C. Papatriantafyllopoulou, A. Terzis, C. P. Raptopoulou, A. Escuer and S. P. Perlepes, *Dalton Trans.* 2010, **39**, 8603; b) S. R. Bayly, Z. Xu, B. O. Patrick, S. J. Rettig, M. Pink, R. C. Thompson and C. Orvig, *Inorg. Chem.* 2003, **42**, 1576.

16 a) Z. Xu, P. W. Read, D. E. Hibbs, M. B. Hursthouse, K. M. A. Malik, B. O. Patrick, S. J. Rettig, M. Seid, D. A. Summers, M. Pink, R. C. Thompson and C. Orvig, *Inorg. Chem.* 2000, **39**, 508; b) A. Upadhyay, N. Komatireddy, A. Ghirri, F. Tuna, K. Langley Stuart, K. Srivastava Anant, E. C. Sanudo, B. Moubaraki, S. Murray Keith, J. L. McInnes Eric, M. Affronte and M. Shanmugam, *Dalton Trans* 2014, **43**, 259; c) J.-P. Costes, T. Yamaguchi, M. Kojima and L. Vendier, *Inorg. Chem.* 2009, **48**, 5555; d) T. Shiga, N. Ito, A. Hidaka, H. Okawa, S. Kitagawa and M. Ohba, *Inorg. Chem.* 2007, **46**, 3492; e) C. A. Barta, S. R. Bayly, P. W. Read, B. O. Patrick, R. C. Thompson and C. Orvig, *Inorg. Chem.* 2008, **47**, 2280; f) V. Chandrasekhar, B. M. Pandian, R. Boomishankar, A. Steiner, J. J. Vittal, A. Houri and R. Clerac, *Inorg. Chem.* 2008, **47**, 4918.

17 N. Ahmed, C. Das, S. Vaidya, A. K. Srivastava, S. K. Langley, K. S. Murray and M. Shanmugam, *Dalton Trans.* 2014, **43**, 17375.

18 a) I. A. Gass, B. Moubaraki, S. K. Langley, S. R. Batten and K. S. Murray, *Chem. Commun.* 2012, **48**, 2089; b) S. K. Langley, B. Moubaraki and K. S. Murray, *Inorg. Chem.* 2012, **51**, 3947; c) H. Tian, Y.-N. Guo, L. Zhao, J. Tang and Z. Liu, *Inorg. Chem.* 2011, **50**, 8688; d) H. Tian, L. Zhao, Y.-N. Guo, Y. Guo, J. Tang and Z. Liu, *Chem. Commun.* 2012, **48**, 708.

19 a) M. Andruh, I. Ramade, E. Codjovi, O. Guillou, O. Kahn and J. C. Trombe, *J. Am. Chem. Soc.* 1993, **115**, 1822; b) C. Benelli, A. Caneschi, D. Gatteschi, O. Guillou and L. Pardi, *Inorg. Chem.* 1990, **29**, 1750; c) T. D. Pasatoiu, J.-P. Sutter, A. M. Madalan, F. Z. C. Fellah, C. Duhayon and M. Andruh, *Inorg. Chem.* 2011, **50,** 5890; d) V. Chandrasekhar, P. Bag, W. Kroener, K. Gieb and P. Muller, *Inorg. Chem.* 2013, **52**, 13078; e) K. C. Mondal, G. E. Kostakis, Y. Lan, W. Wernsdorfer, C. E. Anson and A. K. Powell, *Inorg. Chem.* 2011, **50**, 11604; f) S. Sakamoto, T. Fujinami, K. Nishi, N. Matsumoto, N. Mochida, T. Ishida, Y. Sunatsuki and N. Re, *Inorg. Chem.* 2013, **52**, 7218; g) E. Colacio, J. Ruiz-Sanchez, F. J. White and E. K. Brechin, *Inorg. Chem.* 2011, **50**, 7268; h) M. Towatari, K. Nishi, T. Fujinami, N. Matsumoto, Y. Sunatsuki, M. Kojima, N. Mochida, T. Ishida, N. Re and J. Mrozinski, *Inorg. Chem.* 2013, **52**, 6160.

20 S. K. Singh, N. K. Tibrewal and G. Rajaraman, *Dalton Trans.* 2011, **40**, 10897.

21 A. Upadhyay, C. Das, S. N. Meera, S. K. Langley, K. S. Murray and M. Shanmugam, *J. Chem. Sci.* 2014, **126**, 1443.

22 N. F. Chilton, R. P. Anderson, L. D. Turner, A. Soncini and K. S. Murray, *J. Comput. Chem.* 2013, **34**, 1164.

23 a) W. T. Cartere and S. K. Verley, *Coordination chemistry research progress*, Nova Science, 2008, p247-341; b) S. K. Singh, T. Gupta, P. Badkur and G. Rajaraman, *Chem. Eur. J* 2014, **20**, 10305-10313; c) J. Titis and R. Boca, *Inorg. Chem.* 2010, **49**, 3971-3973.

24 a) A. Upadhyay, S. K. Singh, C. Das, R. Mondol, S. K. Langley, K. S. Murray, G. Rajaraman and M. Shanmugam, *Chem. Commun.* 2014, **50**, 8838; b) G. Cucinotta, M. Perfetti, J. Luzon, M. Etienne, P.-E. Car, A. Caneschi, G. Calvez, K. Bernot and R. Sessoli, *Angew. Chem., Int. Ed.* 2012, **51**, 1606; c) C. Das, A. Upadhyay, S. Vaidya, S. K. Singh, G. Rajaraman and M. Shanmugam, *Chem. Commun.* 2015, **51**, 6137.

25 N. F. Chilton, D. Collison, E. J. L. McInnes, R. E. P. Winpenny and A. Soncini, *Nat. Commun.* 2013, **4**, 3551.

26 a) X. Yi, K. Bernot, O. Cador, J. Luzon, G. Calvez, C. Daiguebonne and O. Guillou, *Dalton Trans.* 2013, **42**, 6728; b) L. J. Batchelor, I. Cimatti, R. Guillot, F. Tuna, W. Wernsdorfer, L. Ungur, L. F. Chibotaru, V. E. Campbell and T. Mallah, *Dalton Trans.* 2014, **43**, 12146; c) J. Jung, F. Le Natur, O. Cador, F. Pointillart, G. Calvez, C. Daiguebonne, O. Guillou, T. Guizouarn, B. Le Guennic and K. Bernot, *Chem. Commun.* 2014, **50**, 13346; d) J. J. Baldovi, J. M. Clemente-Juan, E. Coronado and A. Gaita-Arino, *Inorg. Chem.* 2014, **53**, 11323; e) D. Aravena and E. Ruiz, *Inorg. Chem.* 2013, **52**, 13770.

27 a) R. Orbach, *Proc. R. Soc. London, Ser. A* 1961, **264**, 458; b) E. Lucaccini, L. Sorace, M. Perfetti, J.-P. Costes and R. Sessoli, *Chem. Commun.* 2014, **50**, 1648; c) N. Ishikawa, M. Sugita, T. Ishikawa, S. Koshihara and Y. Kaizu, *J. Phys. Chem. B* 2004, **108**, 11265.

28 a) M. A. Palacios, R. McLellan, C. M. Beavers, S. J. Teat, H. Weihe, S. Piligkos, S. J. Dalgarno and E. K. Brechin, *Chem. - Eur.*

J. 2015, **21**, 11212; b) D. N. Woodruff, F. Tuna, M. Bodensteiner, R. E. P. Winpenny and R. A. Layfield, *Organometallics* 2013, **32**, 1224; c) Z.-S. Meng, F.-S. Guo, J.-L. Liu, J.-D. Leng and M.-L. Tong, *Dalton Trans.* 2012, **41**, 2320; d) C. Das, S. Vaidya, T. Gupta, J. Frost, M. Righi, Mattia, K. Brechin Euan, M. Affronte, G. Rajaraman and M. Shanmugam, *Chem. Eur. J.* 2015, **44**, 15639-15650.

29 A. Upadhyay, S. Vaidya, V. S. Venkatasai, P. Jayapal, A. K. Srivastava, M. Shanmugam and M. Shanmugam, *Polyhedron* 2013, **66**, 87.